Local lattice distortion during the spin-state transition in $LaCoO_3$

S. Yamaguchi, Y. Okimoto, and Y. Tokura*
Department of Applied Physics, University of Tokyo, Tokyo 113, Japan
(Received 16 December 1996)

Infrared spectroscopy of a $LaCoO_3$ crystal has revealed anomalous splitting of the phonon modes as well as their intensity variation with temperature during the spin-state transition. The observed results can be interpreted in terms of local lattice distortion arising from the Jahn-Teller effect of the thermally excited intermediate-spin ($S=1$) state of Co^{3+} ions. A possible role of the e_g orbital ordering is discussed with the analysis of the intensity variation of the split Co−O stretching modes. [S0163-1829(97)50814-9]

The thermally induced spin-state and subsequent nonmetal-metal transitions in perovskite-type cobalt oxide $LaCoO_3$ (Refs. 1–8) have been of considerable interest, yet remain far from being completely understood. The ground state of $LaCoO_3$ is a nonmagnetic insulator. Co^{3+} ions take nominally the $3d^6$ configuration and the spin state is the singlet ($t_{2g}^6:S=0$) due to the crystal-field splitting ($10Dq$) slightly larger than the Hund's-rule coupling.[3] $LaCoO_3$ exhibits an abrupt increase of magnetic susceptibility at 50 −100 K which had been interpreted as a transition from the low-spin (LS) to thermally excited high-spin (HS) state ($e_g^2t_{2g}^4:S=2$) with a spin-gap energy of 0.02−0.03 eV.[7,8] With a further increase of temperature, electrical conduction of $LaCoO_3$ shows a crossover around 500 K from a thermally activated semiconductor to a conductor with metallic resistivity ($\approx 1\times10^{-3}$ Ω cm).[7] Recent neutron-scattering measurements have shown that this nonmetal-metal crossover behavior has no magnetic origin.[9] The important aspect of the electronic property is that the magnitude of the charge gap ($\geqslant$ 0.1 eV)[7] is much larger than that of the spin gap (0.02−0.03 eV) and also than the energy scale of semiconductor-metal crossover temperature ($k_BT_{IM}\approx$ 0.05 eV).[10] This is contrasted to the case of the nonmagnetic $3d$ compound FeSi,[11,12] in which both the spin- and charge-gap energies are comparable ($\approx$ 0.06 eV).

Concerning the nature of the spin-state transition in $LaCoO_3$, there have been some arguments : Investigations of polarized neutron scattering[6] and Knight shift[13] have confirmed that the abrupt increase of magnetic susceptibility is due to the change of the spin state in the Co^{3+} ions. Photoemission studies,[14] however, indicated that the transition could hardly be interpreted in terms of the LS-HS transition and the possibility of the intermediate-spin (IS) state ($e_g^1t_{2g}^5:S=1$) as the high-temperature state has also been proposed.[15] More lately, using the LDA+U approach, Korotin *et al.*[16] have shown that the IS state is energetically comparable to the LS state, but much more stabilized than the HS state due to the larger p-d hybridization as well as the orbital-ordering effect. One of the important consequences of such an IS model is that the thermally excited $S=1$ species should be subject to Jahn-Teller (JT) distortion arising from the orbital degeneracy of the e_g state. Thus, we may expect the onset of dynamical JT distortion in accord with evolution of the LS-IS transition, which may not be detected by diffraction measurements as an averaged structure but by the measurement of phonon spectra probing the dynamical and local lattice change. This is the motivation of the present paper.

$LaCoO_3$ crystals and Sr-doped crystals ($La_{1-x}Sr_xCoO_3$) were grown by the floating-zone method, the details of which have been published in Refs. 7 and 10. The powder-diffraction x-ray pattern showed that the sample of $LaCoO_3$ is a slightly distorted perovskite with rhombohedral structure ($R3c$), consistent with the result of the literature.[17] The analysis of composition was carried out using an electron probe microanalyzer (EPMA), indicating the nearly identical composition with the prescribed one. Magnetization measurements were done with a commercial superconducting quantum interference device (SQUID) magnetometer. Measurements of reflectivity spectra were done for the photon energy region between 0.02 and 35 eV on a specularly polished surface of the crystal using Fourier spectroscopy (0.02 −0.8 eV) and grating spectroscopy (0.6−35 eV). The reflectivity data above 6 eV, which was necessary to execute the accurate Kramers-Kronig (K-K) transformation, were obtained using a synchrotron radiation at INS-SOR, Institute for Solid State Physics, University of Tokyo, as a light source. Temperature-dependent reflectivity spectra at 0.02−6 eV were connected to the room-temperature data of reflectivity (6−35 eV) and the spectra of the dielectric constant were deduced by the K-K analysis.

We show in Fig. 1(a) temperature dependence of magnetic susceptibility for $LaCoO_3$, that shows a similar behavior as previously reported.[4,7] The susceptibility has an abrupt decrease at 50−100 K although accompanied with a small Curie-like contribution from impurities below 20 K. We subtracted the effects of impurities (or slight oxygen nonstoichiometry) to show the susceptibility for the hypothetically stoichiometric crystal (closed circles). Above 150 K, the magnetic susceptibility shows paramagnetic behavior. In order to analyze the spin state, we have adopted the two-level model; the thermally excited IS (or HS) state from the LS ground state split by the spin-gap energy Δ and with the exchange energy J between excited neighboring spins as described in Ref. 7. With use of the simple molecular-field approximation, we obtained the best-fitted results for IS (solid line) and HS (dashed line) models, respectively, as shown in Fig. 1(a). Both results well reproduce the experimental result at 2−120 K, yet there are certain discrepancies above 120 K, implying further complexity in the electronic

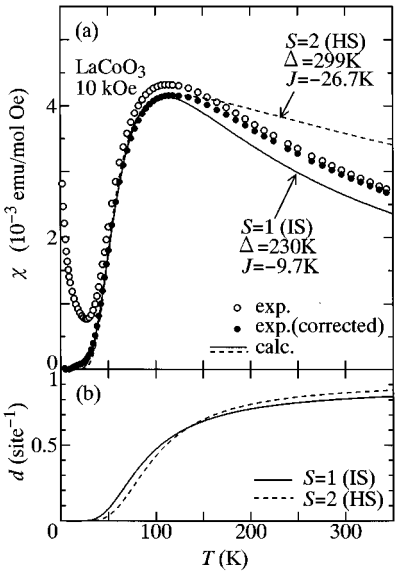

FIG. 1. (a) Magnetic susceptibility χ (open circles) and the corrected one (closed circles) by the subtraction of the contribution from Curie-like impurities. Results of the curve fitting are shown on the basis of the molecular-field approximation with an energy level separation Δ between the $S=0$ (LS) and $S=1$ (IS) (a solid line) and between the $S=0$ (LS) and $S=2$ (HS) (a dashed line), respectively, with the antiferromagnetic interaction (J) between the neighboring IS or HS Co ions (see text). (b) The mean density d of the thermally excited IS (solid line) or HS (dashed line) states calculated with the same parameters as used in the fitting of χ.

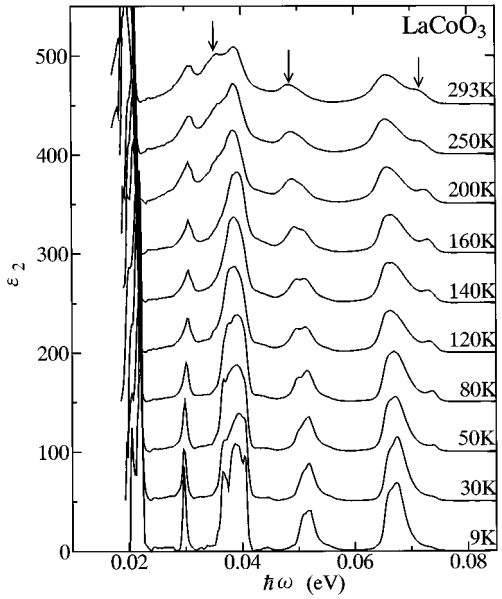

FIG. 2. Temperature dependence of optical phonon spectra. Arrows exemplify the extra modes of phonons appearing only in the high-temperature spin state. The respective spectra are vertically offset by every 50 of ε_2 for clear comparison.

structure that is not explained by such a simple spin-state transition. In Fig. 1(b), we show the mean IS (or HS) density per Co site, which equals the probability to find the magnetic ion at a Co site, calculated using the parameters in Fig. 1(a). For both cases, over 80% of Co ions are already excited to magnetic states at room temperature.

To detect possible local-structural change during such a spin-state transition, we have investigated the temperature dependence of optical phonon spectra (Fig. 2). There are three major peaks at around 0.022, 0.039, and 0.067 eV and additionally two smaller peaks at around 0.030 and 0.051 eV. At a glance, the respective peaks shift slightly to lower energy and are gradually broadened with increase of temperature. Furthermore, new growth of extra phonon modes is observed, as exemplified by arrows. The group theory predicts eight infrared-active phonon modes for the perovskite-type structure with rhombohedral distortion D_{3d}^6 ($R\bar{3}c$) (Ref. 18); $3(A_{2u}+E_u)+2E_u$. Here the coefficient in the first term corresponds to the three vibration modes in the cubic lattice, namely the so-called external, bending, and stretching modes, as schematically illustrated in Fig. 10 of Ref. 18. The respective modes are degenerated in the cubic lattice, but the degeneracy is lifted ($A_{2u}+E_u$) by rhombohedral distortion. The $2E_u$ modes are allowed by the folding of the Brillouin-zone boundary due to doubling of the cubic unit cell. According to the mode classification[18] and the analysis of the room-temperature spectra,[19] we have assigned the three major peaks to, from low to high energy, the external, bending, and stretching modes, respectively, and two small peaks to the zone-folded modes. Neutron-diffraction measurements[17] have shown that in this temperature range there is no lattice distortion (in the sense of static and long-range order) other than the rhombohedral one which gradually decreases and approaches the cubic symmetry with increase of temperature. Thermal expansion of the unit cell (without change of symmetry) should cause the temperature-dependent shift of phonon peaks,[20] but cannot explain unusual growth of the extra modes (arrows) as observed in the respective frequency regions of the bending (0.035 eV), stretching (0.073 eV), and Brillouin-zone-folded mode (0.050 eV). These phonon anomalies should then be ascribed to local lattice distortion which had previously not been detected by diffraction measurements but must be relevant to the spin-state transition.

We performed the dispersion analysis on the spectra of the stretching modes (0.067 eV) which are well separated from and hence least affected by the other spectral structures. We have used three Lorentzian oscillators, as shown in Fig. 3(a), to fit the observed spectra by the least-square method. Temperature dependencies of the oscillator strengths of the respective bands (S_1, S_2, and S_3) are plotted with closed circles in Fig. 3(b). Distinct changes in the respective oscillator strengths are observed in the temperature range of 50 -150 K where the magnetic susceptibility exhibits a steep change. The phonon modes under consideration correspond to the vibration of O^{2-} ion along the Co$-$O$-$Co bond direction and hence should be sensitive to the Co$-$O$-$Co bond covalency. Mode S_1 decreases its intensity with temperature, while the S_2 and S_3 bands are enhanced. Therefore, the S_1 mode should be relevant to motion of the oxygen adjacent to the LS Co site, while the Co$-$O$-$Co bonds corresponding to the S_2 and S_3 modes must contain (at least one) IS (or HS) Co site(s).

To investigate the origin of the local lattice distortion induced by the spin-state transition, we have analyzed the result of Fig. 3 in terms of the two (A and B) models shown in Fig. 4 : In model A, we assign the three modes (S_1, S_2, and

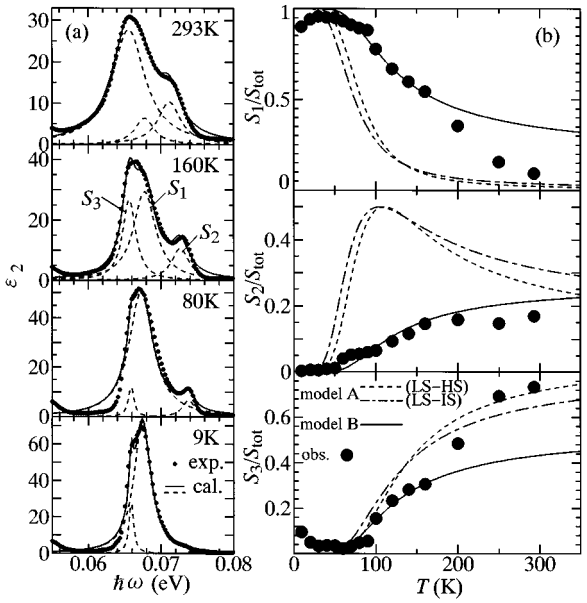

FIG. 3. (a) Magnified spectra of the stretching-mode phonons (dots) and the best-fitted results (solid lines) with three Lorentzian oscillators S_1, S_2, and S_3 (dashed lines). (b) Temperature dependence of the oscillator strength of each mode (closed circles) normalized to the total strength $S_{tot} \equiv S_1 + S_2 + S_3$. Dash-dotted (dashed) lines represent the calculated results based on model *A* which takes into account three different bonds made of LS−LS, LS−IS(HS), and IS(HS)−IS(HS). Solid lines stand for the calculated results based on model *B*, in which the orbital-ordered IS states are postulated as a thermal excited configuration (Ref. 16). See text and also Fig. 4.

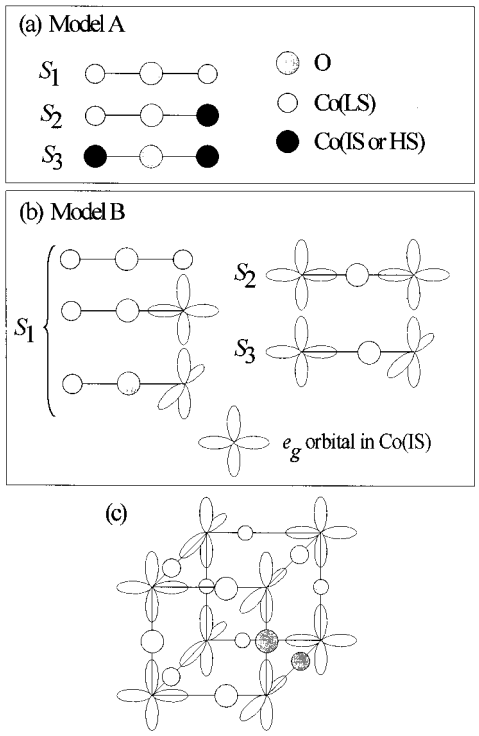

FIG. 4. (a) Model *A* : The local bonds, namely, Co(LS)−O−Co(LS), Co(LS)−O−Co(IS or HS), and Co(IS or HS)−O−Co(IS or HS), are assigned to the stretching phonon modes S_1, S_2, and S_3, respectively, in which the IS or HS species is thermally excited randomly at the respective sites. (b) Model *B*: Three kinds of Co(LS)-containing bonds are assigned to the S_1 mode, and two kinds of Co(IS)−O−Co(IS) bonds in the orbital-ordered IS state to the S_2 and S_3 modes. (c) The orbital-ordered IS state according to the LDA+U calculation (Ref. 16), indicating that the intensity ratio of S_2 to S_3 in model *B* equals 1:2.

S_3), as shown in Fig. 4 (a), to the three kinds of local bonds, namely Co(LS)−O−Co(LS), Co(LS)−O−Co(IS or HS), and Co(IS or HS)−O−Co(IS or HS). We may neglect the effect of the rhombohedral distortion and its temperature variation on the presently observed mode splitting. Here we postulate that either the IS or HS species is thermally excited randomly at the respective sites. Then, the number of the respective bonds are given as $(1-d)^2$, $d(1-d)$, and d^2, d being the IS (or HS) density. Provided that the oscillator strength of each mode is simply proportional to the number of the corresponding bonds in the crystal, we show in Fig. 3(b) the calculated results of the temperature dependencies of the relative mode intensity S_i/S_{tot} $(i=1,2,3)$ for the LS −IS (dash-dotted line) and the LS−HS (dashed line) transitions. At a glance, there is a large discrepancy between the observed and calculated results for the S_2 mode. The agreement is obviously not improved even if the mode assignments of S_2 and S_3 are exchanged. Model *A* [Fig. 4(a)] thus fails to explain the observed result.

As an alternative explanation [model *B* shown in Fig. 4(b)], we consider the orbital-ordered IS state accompanied by collective Jahn-Teller distortion[16] as an origin of split modes (S_2 and S_3) in the high-temperature region. In model *B*, we assign the mode S_1 to all the LS-containing bonds. We further assume that the intensity ratio of S_2 to S_3 is 1:2 as in the orbital-ordered state illustrated in Fig. 4(c). Then, the relative mode intensities are given as $S_1/S_{tot} \approx 1-d^2$, $S_2/S_{tot} \approx d^2/3$, and $S_3/S_{tot} \approx 2d^2/3$. The calculated results based on model *B* [Fig. 4(b)] are shown by solid lines in Fig. 3(b). Model *B* can account for the overall features of the experimental observation below 160 K, although some discrepancy becomes evident above 200 K. Within the framework of the orbital-ordered IS, we may have to consider the correlation between the IS sites arising from the orbital-ordering effect as well as the increasing thermal fluctuation or melting of the orbital order[16] at high temperatures. The correct statistics for the orbital ordering and the bond configuration dependence of the oscillator strength of the phonon mode should be taken into account for further quantitative argument.

In summary, remarkable splitting and intensity variation of the phonon modes have been found during the spin-state transition in $LaCoO_3$. The local lattice distortion, which perhaps arises from the Jahn-Teller distortion of the thermally excited intermediate-spin $(S=1)$ state in Co^{3+} ions, is responsible for this anomalous behavior of the phonon modes. A possible role of the (short-range) ordering of the e_g orbital has been pointed out in terms of the analysis of the temperature dependence of the intensities of the split oxygen phonon modes.

This work was in part supported by a Grant-In-Aid for Scientific Research from the Ministry of Education, Science and Culture, Japan, and also by New Energy and Industrial Technology Development Organization (NEDO).

*Author to whom correspondence should be addressed.
[1] R. R. Heikes, R. C. Miller, and R. Mazelsky, Physica (Amsterdam) **30**, 1600 (1964).
[2] C. S. Naiman, R. Gilmore, B. DiBartolo, A. Linz, and R. Santoro, J. Appl. Phys. **36**, 1044 (1965).
[3] P. M. Raccah and J. B. Goodeneough, Phys. Rev. **155**, 932 (1967).
[4] V. G. Bhide, D. S. Rajoria, G. R. Rao, and C. N. R. Rao, Phys. Rev. B **6**, 1021 (1972).
[5] G. Thornton, B. C. Tofield, and D. E. Williams, Solid State Commun. **44**, 1213 (1982).
[6] K. Asai, P. Gehring, H. Chou, and G. Shirane, Phys. Rev. B **40**, 10 982 (1989).
[7] S. Yamaguchi, Y. Okimoto, H. Taniguchi, and Y. Tokura, Phys. Rev. B **53**, R2926 (1996).
[8] M. Itoh and I. Natori, J. Magn. Magn. Mater. **140-144**, 2145 (1995).
[9] K. Asai, O. Yokokura, N. Nishimori, H. Chou, J. M. Tranquada, G. Shirane, S. Higuchi, Y. Okajima, and K. Kohn, Phys. Rev. B **50**, 3025 (1994).
[10] S. Yamaguchi, Y. Okimoto, and Y. Tokura, Phys. Rev. B **54**, R11 022 (1996).
[11] Z. Schlesinger *et al.*, Phys. Rev. Lett. **71**, 1748 (1993).
[12] P. Nyhus, S. L. Cooper, and Z. Fisk, Phys. Rev. B **51**, 15 626 (1995).
[13] M. Itoh, M. Sugahara, I. Natori, and K. Motoya, J. Phys. Soc. Jpn. **64**, 3967 (1995).
[14] M. Abbate, J. C. Fuggle, A. Fujimori, L. H. Tjeng, C. T. Chen, R. Potze, G. A. Sawatzky, H. Eisaki, and S. Uchida, Phys. Rev. B **47**, 16 124 (1993).
[15] R. H. Potze, G. A. Sawatzky, and M. Abbate, Phys. Rev. B **51**, 11 501 (1995).
[16] M. A. Korotin, S. Y. Ezhov, I. V. Solovyev, V. I. Anisimov, D. I. Khomskii, and G. A. Sawatzky, Phys. Rev. B **54**, 5309 (1996).
[17] G. Thornton, B. C. Tofield, and A. W. Hewat, J. Solid State Chem. **61**, 301 (1986).
[18] M. D. Fontana, G. Métrat, J. L. Servoin, and F. Gervais, J. Phys. C **16**, 483 (1984).
[19] S. Tajima, A. Masaki, S. Uchida, T. Matsuura, K. Fueki, and S. Sugai, J. Phys. C **20**, 3469 (1987).
[20] S. S. Mitra *et al.*, Phys. Rev. Lett. **18**, 455 (1967).